Dielectrophoresis-Based Classification of Cells Using Multi-Target Multiple-Hypothesis Tracking

Samuel J. Dickerson, Donald M. Chiarulli, Steven P. Levitan, Craig Carthel and Stefano Coraluppi

***Abstract*— In this paper we present a novel methodology for classifying cells by using a combination of dielectrophoresis, image tracking and classification algorithms. We use dielectrophoresis to induce unique motion patterns in cells of interest. Motion is extracted via multi-target multiple-hypothesis tracking. Trajectories are then used to classify cells based on a generalized likelihood ratio test. We present results of a simulation study and of our prototype tracking the dielectrophoretic velocities of cells.**

I. Introduction

In recent years, there has been growing interest in the use of dielectrophoresis as a means to characterize and identify cells [1]. To date, this characterization has remained a manual process where observations of cells undergoing dielectrophoresis are made under a microscope and cell velocities are individually recorded. Such a laborious process becomes impractical once the cell population is large, as is the case with the cell and bacteria samples used in medical diagnostics and has prevented dielectrophoresis from being used in practical applications. In our work, we leverage recent advancements made in the area of object tracking to be able automatically collect dielectrophoresis velocity data to overcome this problem [2, 3]. When combined with algorithms for statistically classifying the cell tracks, we provide a unique platform for rapidly identifying cell types in heterogeneous mixtures.

Our approach is based on the combination of three technologies (Figure 1): dielectrophoresis, where AC electric fields can be used to induce motion in cells; multi-target tracking algorithms that capture cell trajectories; and statistical classification algorithms that differentiate cells based on observed motion characteristics. Together these three technologies provide a unique ability to identify specific particles from a library of pre-characterized species. The existence of certain particle types (e.g., pathogens) can be identified even when there are a relatively small number of particles of interest present in the sample. Our methodology has the potential to reduce the time to process diagnostics by orders of magnitude as cells respond to changes in dielectrophoresis fields nearly instantaneously, causing the identification turnaround time to be bounded by computation rather than waiting on biological processes such as amplification of cell colonies in a culture medium.

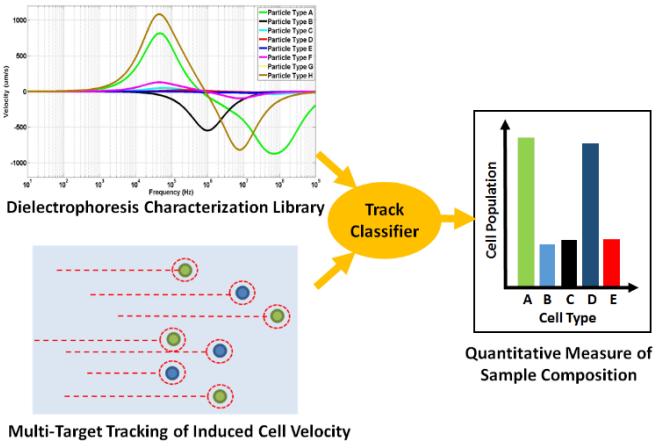

Figure 1. Cell classification methodology.

II. Cell Classification Approach

In this section we describe the three facets of our approach: Dielectrophoresis, multi-target tracking and classification of tracks and how they are used in tandem to identify cells.

A. Dielectrophoresis Induced Motion of Cells

Dielectrophoresis is a technique where spatially non-uniform AC electric fields can be used to exert force on a particle. The magnitude and direction of the force is highly dependent upon the electrical properties of the particle. The form of dielectrophoresis we employ (although not limited to) is traveling wave dielectrophoresis. Typically, traveling-wave configurations employ a linear electrode array as shown in Figure 2(a). The time-averaged force exerted on a particle undergoing traveling-wave dielectrophoresis as a result of such an electrode arrangement is given by [4]:

$$\langle \vec{F}_{DEP} \rangle = 2\pi\varepsilon_m r^3 \left[Re(K_{CM})\nabla E_y^2 + Im(K_{CM})E_x^2 \nabla\phi_x \right] \quad (1)$$

$$K_{CM} = \frac{\varepsilon_p^* - \varepsilon_m^*}{\varepsilon_p^* + 2\varepsilon_m^*} \quad (2)$$

where r is the radius of the particle, ε_p and ε_m are the electrical permittivities of the particle and surrounding medium, and E is the electric field that is at phase ϕ. The frequency dependent Clausius-Mossotti factor, K_{CM}, is the key to the selective capabilities of dielectrophoresis. The real part of K_{CM} acts as a proportionality constant to the vertical component of force exerted on the particle (DEP), while the imaginary part of K_{CM} acts on the lateral force component (TWDEP). Figure 2(b) shows the velocity

Samuel J. Dickerson is with Nanophoretics LLC, Monroeville, PA 15146 USA (e-mail: sam@nanophoretics.com).

Donald M. Chiarulli and Steven P. Levitan are with the University of Pittsburgh, Pittsburgh, PA 15260 USA, in the departments of Computer Science and Electrical and Computer Engineering (e-mail: don@cs.pitt.edu and levitan@pitt.edu).

Craig Carthel and Stefano Coraluppi are with Systems & Technology Research, Woburn, MA 01801 USA.

978-1-4244-7929-0/14/$26.00 ©2014 IEEE

spectra for a model cell population containing viable and non-viable yeast cells. The appeal of dielectrophoresis in our method is that the force components can be measured indirectly by configuring a known electric field and recording the particle's velocity. If these observations are made over a wide frequency range, the unique responses of the particles within the population can be extracted. In our approach, extraction of this data takes place automatically by way of advanced multi-target tracking algorithms.

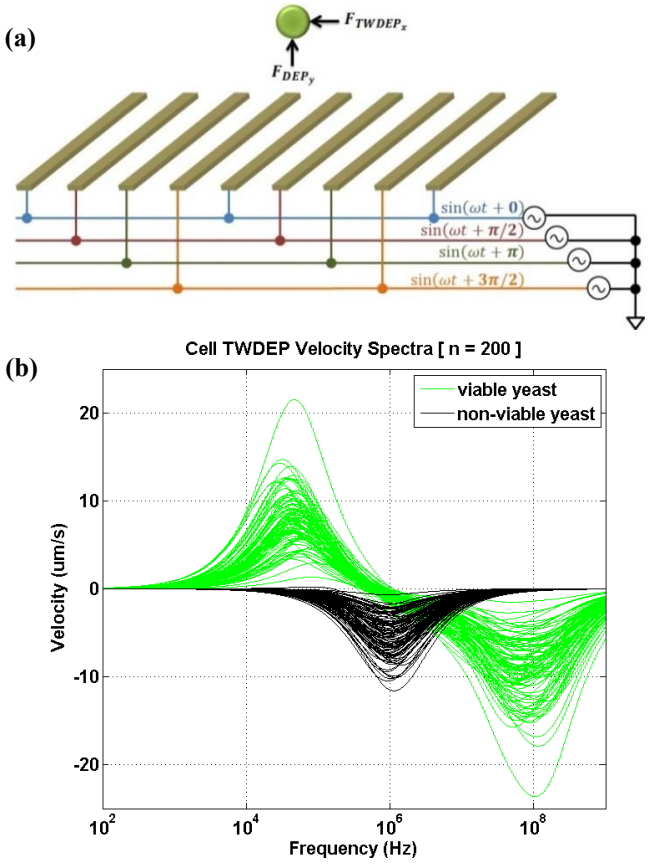

Figure 2(a) Cell undergoing traveling-wave dielectrophoresis (b) TWDEP velocity spectra for mixed population of viable and non-viable yeast cells

B. Multi-Target Multiple Hypothesis Cell Tracking

Simultaneously tracking the trajectories of multiple objects is a difficult, computationally intensive problem to solve and is currently the subject matter of much research for defense surveillance applications. Multi-target tracking (MTT) algorithms are fundamentally different from single-target algorithms in that they must be able to accommodate cases in which there may be an unknown number of targets, targets that are closely spaced together and targets having paths that cross over one another. Such is the case when thousands of cells are moving together under the influence of dielectrophoresis. This presents a data association problem in which one is given a sequence of sets of track measurements, and must determine which measurements to associate with which targets and which to discard. For this cell tracking application, our solution includes particle detection based on advanced image-segmentation and feature-aided MTT where the augmented state space includes both target kinematics and detection-level features such as particle size, shape and color.

Multiple-hypothesis tracking (MHT) is generally acknowledged as the most powerful paradigm for multi-target tracking [5]. Hypothesis-oriented methods can lead to an unmanageable number of hypotheses even for a small number of objects. We employ a computationally-efficient, multi-stage MHT implementation that builds upon the track-oriented approach without having to do a costly enumeration of global hypotheses [3].

For a sequence of targets observations $z_k = (z_1,\ldots,z_k)$, we wish to estimate the state history X^k for all objects present in the surveillance region that exist over the time sequence $(t_1,\ldots,\ t_k)$ given the auxiliary discrete state history q^k that represents of all contact data: which contacts are false, how the tracks are to be associated, and when objects are born and die. We are interested in the probability distribution $p(\ X^k \mid Z^k)$ for object state histories given data. This quantity can be obtained by conditioning over all possible auxiliary states histories q^k.

$$p\left(X^k \mid Z^k\right) = \sum_{q^k} p\left(X^k \mid Z^k, q^k\right) p\left(q^k \mid Z^k\right) \tag{3}$$

The MHT approach seeks to identify the *maximum a posteriori probability* (MAP) estimate for the auxiliary state history q^k, and identify the corresponding *minimum mean square error* (MMSE) estimate for the object state history X^k conditioned on the estimate for q^k,

$$\hat{q}^k = \arg\max_{q^k} p\left(q^k \mid Z^k\right) \tag{4}$$

$$\hat{X} = \hat{X}_{MMSE}\left(Z^k, \hat{q}^k\right) \tag{5}$$

Rather than reasoning over all of the global hypotheses q^k, a set of trees is maintained that represents the local hypotheses for detected targets. To resolve the hypotheses (i.e. determine trajectory of a cell), we select the set of tree leaves that correspond to the MAP solution (4), with the constraint that all measurements are utilized at most once. This hypothesis resolution entails solving an integer programming problem by way of linear programming and Lagrangian relaxation. This approach allows us to identify a near-optimal global hypothesis of the cell trajectories without explicitly enumerating all of the candidate hypotheses, which would quickly become intractable.

C. Classification of Cell Tracks

The classification goal is to identify the presence or absence of a targeted cell type in a mixed sample based the tracked features. The feature set for each object includes the velocity components at a sequence of excitation frequencies, as well as static feature states (cell color and geometry). It is important to note that the actual dielectrophoresis field configuration parameters are not explicitly encoded in the feature set. Instead, training data sets for a given cell type are obtained by exposing samples of known composition to a

predefined sequence of fields. Subsequently, trajectories from an arbitrary mixture of cell types are scored with respect to each calibrated type.

Tracks are classified based on the *generalized likelihood ratio test* (GLRT) [6]. The calibration equations used are:

$$\mu_{i,j} = \frac{1}{N}\sum_{N_{tracks}} X_s \tag{6}$$

$$\Sigma^2_{i,j} = \frac{1}{N-1}\sum_{N_{tracks}} \left(X_s - \mu_{i,j}\right)^2 \tag{7}$$

First, the hypothesis (H_i) that best explains the observations is generated by determining what the maximum-likelihood cell type is for each cell track. Then, the probability of that hypothesis is tested against the null hypothesis (H_0), that the tracking data could be better explained as resulting from a general type we refer to as *'other'*, a type for which there is no corresponding model or training data available. H_0 must be sufficiently distinct from H_i in order to reasonably determine the cell type. A bounding region is introduced around H_i and the restriction $\Sigma > \Sigma_{min}$ is maintained so as to avoid degeneracy, as more likely hypotheses corresponding to type *'other'* can always be generated.

$$p(z|H_i) = N(z;\mu_i,\Sigma_i) \tag{8}$$

$$p(z|H_0) = \max_{\mu \notin \cup_i [\mu_i-\Delta\ \mu_i+\Delta\ ], \Sigma > \Sigma_{min}} \left(N(z;\mu,\Sigma) \right) \tag{9}$$

Classification based on comparisons to calibrated training data, versus solely on models, is advantageous in real-world experimental settings where there are difficult to predict, but deterministic, factors to contend with such as AC electroosmosis [7] and unknown medium conductivities. These factors cause significant deviations from model predictions. An additional advantage of GLRT in this application is that it provides accurate results without prior knowledge of the distribution of cell types in the mixture, which is precisely the parameter we wish to determine.

III. Results

In this section we first present results of a simulation-based study on the effectiveness and that of our experimental setup being used to track yeast cells.

A. Simulation Results

In order to evaluate our methodology, we carried out extensive simulation-based testing. The physics were modeled using well-established multi-shell models for viable and non-viable yeast cells [8]. In order to capture the diversity that occurs even within a given cell type, the cell model parameters were allowed to vary randomly, resulting in a sample population with multiple overlapping spectra, as seen in figure 2(b). Image processing is simulated with a fixed detection probability, location and feature measurements with additive Gaussian noise and uniformly distributed false alarms in the imaging space.

The simulation of figure 3(a) begins with a training phase on viable and non-viable yeast samples, each containing 200 cells. Six examination frequencies between 1 kHz and 100 MHz are cycled at fixed durations and MHT is used to capture the dielectrophoresis induced trajectories of the cells. Subsequently, this process is repeated for an arbitrary mix of 200 cells during the testing phase. A *nearly-constant velocity Kalman* smoothing filter is used to smooth the tracks before GLRT classification. Figure 3(b) shows an overlay of all the cell trajectory x-components during the testing phase, both before and after filtering.

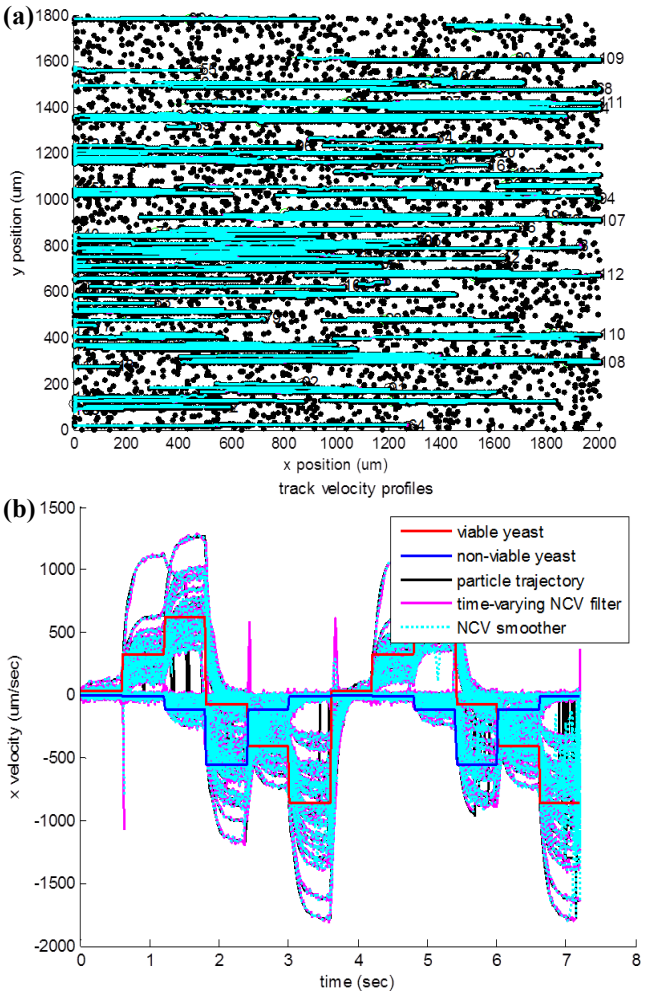

Figure 3(a). Simulated positional trajectories of yeast cell mixture (selected cell tracks highlighted) (b) Overlay of all cell velocity trajectories during testing phase

Table 1. GLRT Classifier Output

	viable yeast	non-viable yeast	"other"
Ground truth	96	104	0
raw MHT output	122	109	7
lifetime-based aggregation	71	74	2
concurrency-based aggregation	92	97	4

Table 1 shows the results of GLRT classification of the simulated tracks. Automatic tracking algorithms incur track fragmentation errors, therefore two track aggregation

schemes were considered to reduce the number of declared tracks. The *lifetime-based aggregation* scheme computes the ratio of the sum of track lifetimes to total scenario duration for each type. The concurrency-based aggregation scheme calculates the maximum number of tracks of each type in existence at any time. Both aggregation schemes improve the performance of the MHT tracker.

B. *Experimental Multi-Target Tracking of Cells*

To date, we have designed and constructed a hardware platform with the ability to dielectrophoretically manipulate cells, record image data and track the cell motion. In experimental settings, particle-detection processing is more complex than what is required for synthetic datasets. Thus, we applied image-segmentation algorithms from which only those elements were extracted for which dimensions were roughly consistent with yeast cell sizes.

Figure 4 shows data from a target tracking experiment using a sample of yeast cells on our experimental platform. The MHT algorithm analyzed 2,000 consecutive image frames from the microscope camera. Figure 4(a) shows the cells before the fields is activated. Figure 4(b) shows the track history of each cell superimposed on a single frame from the camera movie. Figure 4(c) is a histogram of instantaneous cell velocities after a 250 kHz traveling wave dielectrophoresis field was applied for 12 seconds.

As shown by cell models of Figure 2 and the histogram of Figure 4(c), at 250 kHz non-viable yeast cells have a very small force exerted on them while viable cells have a large induced velocity. The histogram shows that the majority of viable cells move from left to right, centered on a mean velocity of 5um/s. The peak shown near 0 um/s is a combination of non-viable cell tracks and other zero velocity false tracks that are not filtered out. Further work is ongoing to incorporate the ability to extract ground-truth from these scenarios and allow that the performance of GLRT classification scheme to be formally verified.

IV. Conclusion

We have proposed a novel methodology for classifying cells based on the combined use of dielectrophoresis, multi-target multiple-hypothesis tracking and classification algorithms. As has been shown, the integration of advanced target tracking algorithms and GLRT classification enables dielectrophoresis to be used as a practical diagnostics tool in real-world scenarios where there are samples with high cell concentration and the velocity trajectory of each individual cell must be recorded.

V. References

[1] Pethig, R. "Review Article—Dielectrophoresis: Status of the theory, technology and applications". *Biomicrofluidics* 4, 2010.

[2] Carthel, C. and Coraluppi, S. Particle Tracking Workshop Methods and Results, IEEE International Symposium on Biomedical Imaging – *Particle Tracking Challenge Workshop*, Barcelona, Spain, May 2012.

[3] Carthel, C. and Coraluppi, S. "Multi-Stage Multiple-Hypothesis Tracking", *ISIF Journal of Advances in Information Fusion*, , June 2011.

[4] Wang, XB *et al.* "A unified theory of dielectrophoresis and travelling wave dielectrophoresis" *J. Phys. D: Appl. Phys.* 27 157 1994.

[5] Y. Bar-Shalom, P. Willett, and X. Tian, "Tracking and Data Fusion: A Handbook of Algorithms", YBS Publishing, 2011.

[6] H. V. Poor, An Introduction to Signal Detection and Estimation, Springer-Verlag, 1988.

[7] Castellanos, A. et al. "Electrohydrodynamics and dielectrophoresis in microsystems: scaling laws", *J. Phys. D: Appl. Phys.* , 36. 20, 2003

[8] Hölzel, R. "Electrorotation of single yeast cells at frequencies between 100 Hz and 1.6 GHz". Biophys J.; vol. 73(2), August 1997.

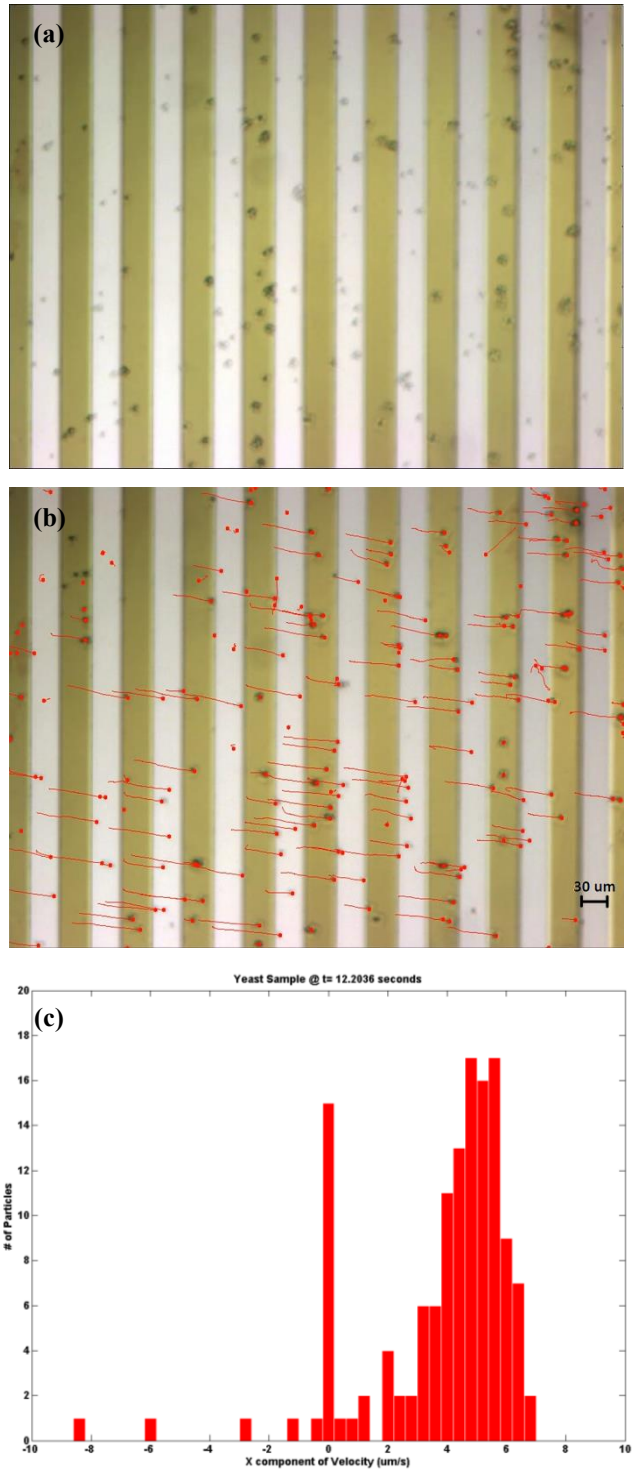

Figure 4(a) Yeast cells above electrodes before activation of dielectrophoresis fields. (b) Cells undergoing dielectrophoresis with super-imposed tracks (c) Histogram of instantaneous velocities of tracked yeast cells within the camera field of view.